



Hillock sizes after wet etching in silicon

D.A. Mirabella, M.P. Suárez, C.M. Aldao*

Institute of Materials Science and Technology (INTEMA), University of Mar del Plata and National Research Council (CONICET), Juan B. Justo 4302, B7608FDQ Mar del Plata, Argentina

ARTICLE INFO

Article history:

Received 30 June 2009

Accepted for publication 21 September 2009

Available online 25 September 2009

Keywords:

Monte Carlo simulations

Etching

Surface structure

Morphology

Roughness and topography

ABSTRACT

The formation of two- and three-dimensional hillocks is regularly observed in Si(1 1 1) steps and Si(1 0 0) during wet etching. Frequently the resulting morphology consists of hillocks scattered on a landscape of limited roughness. Recently we proposed a mean field model (MFM) in which the observed hillock-and-valley pattern is possible under steady state if hillock etching is slightly faster than valley etching. This condition implies that hillock size distributions must be an exponential decreasing function. In this work, we report a systematic study of hillock size distributions of experimental morphologies obtained under different etchant concentrations in Si(1 0 0). We found that experimental hillock size distributions are in agreement with those predicted by the MFM.

© 2009 Elsevier B.V. All rights reserved.

1. Introduction

Anisotropic chemical etching of silicon in aqueous solutions, such as KOH or NH₄OH, is a widely used technique to produce smooth surfaces in micromachining with nanometer precision [1]. Etching is a complex phenomenon that accounts for multiple interrelated processes occurring at the atomic scale. Atomistic processes strongly depend on the interaction between substrate atoms, surface orientation (atom coordination number), etchant composition and concentration, temperature, and possible external perturbation such as stirring. Having this picture in mind, one can expect that more coordinated atoms are etched with a slower rate than those having fewer neighbors. In this context, one can expect that any type of protrusion would be unstable and should tend to disappear leading to a smooth surface. However, surfaces frequently roughen. In particular, the formation of pyramidal etch hillocks has been regularly reported in silicon etching [2–7].

High anisotropic dissolution ratios are very well known since many years ago, with the (1 0 0) and (1 1 0) surfaces dissolving much more rapidly than the (1 1 1) plane [8,9]. Then, etching of vicinal Si(1 1 1) occurs by the continuous retreat of the steps. Thus, the surface morphology is dominated by step roughening since terraces are rarely attacked. When Si(1 1 1) miscut in the $[\bar{1} \bar{1} 2]$ direction is etched, two-dimensional etch hillocks appear giving a shark's tooth shape to the structure with many straight step segments oriented in the $[1 \bar{1} 2]$ that constitute the slow etching step [10]. Si(1 0 0) etching process exposes the more stable (1 1 1) planes that become the sides of pyramidal features. However, it is important to emphasize that the stability of (1 1 1) planes is

not enough to account for the formation of hillocks; in addition, hillock tops must etch slow and the (1 1 1) hillock sidewalls must be stable [11].

To justify or explain the reduction of the etch rate at the top of the hillock, researchers propose external mechanisms such as the appearance of semipermeable or masking particles that adhere to the apex reducing the hillocks etch rate. The exact nature of these masking particles remains under debate but silicate particles [12] and hydrogen bubbles [13] are the most referenced in the literature as possible candidates for this mechanism. Hines and co-workers proposed an alternative explanation to the origin of the hillock apices stability, taking into account factors such as steric hindrance and lattice strain that can play a role in relative site reactivities [10,14,15]. They proposed that the topmost site of a two-dimensional hillock in etching of vicinal Si(1 1 1) is unhindered, unstrained, and then relatively resistant to etching. Also, Gosálvez and Nieminen [16] proposed that the origin of the differences in site-specific etching rates is found in the weakening of backbonds due to OH termination of surface atoms and interactions between the terminating species. This model is very detailed and realistic but it fails in reproducing the hillock-and-valley patterns experimentally observed. Following the work of Hines and co-workers, we found that hillocks as observed in 1D and 2D, can be reproduced with a simple site-specific etching model as they originally proposed for Si(1 1 1) [17–19]. However, we do not claim that the unstrained argument is valid for 2D substrate as the attachment of masking particles can be related to apex formation.

It is important to stress that, depending on the specific conditions, three different regimes concerning the formation of hillocks can occur. These regimes emerge in experiments and modeling: regime I, hillocks do not form; regime II, disjoint hillocks form originating a hillock-and-valley pattern; and regime III, hillocks

* Corresponding author. Tel.: +54 223 4816600; fax: +54 223 4810046.
E-mail address: cmaldao@mdp.edu.ar (C.M. Aldao).

form covering the whole surface (texturized pattern). We will focus here exclusively on regime II.

We have introduced a simple mean field model that predicts the observed morphology and allows us to establish that hillock size densities must be decreasing exponential functions [19]. This finding was also confirmed using a Monte Carlo simulation [18]. In this work we present the hillock size distributions obtained from experimental SEM, results that confirm the validity of our model and discuss the effect of the etchant concentration.

2. Experiments

Samples were cut from a Si wafer that was n-type, P-doped, 4.5 Ω -cm of resistivity, oriented within 0.5° of (1 0 0). Prior to the experiments, the native oxide layer on the silicon was removed by immersion for 2 min in 2 M hydrofluoric acid at room temperature. Samples were then rinsed in tetradistilled water and dried in a flow of N₂. Studies were carried out with samples of about 1 × 1 cm² in a glass cell.

Silicon wafers were supported horizontally in a Teflon holder within a Pyrex vessel mounted on a hot plate stirrer with controlled temperature to within ±1 °C. Wafers were etched in 1, 2, and 4 M KOH solutions until steady state, after the etchant was allowed to reach the desired temperature, then removed from the vessel, rinsed with tetradistilled water and dried in vacuum. The etched crystal surfaces were imaged with a scanning electron microscope (SEM).

Consistently with results reported in Ref. [20], we found that the surface evolves to reach steady state at about 1 h or less. Consequently, samples were etched for 2 h. Fig. 1 shows an SEM image of a Si(1 0 0) surface etched in different KOH concentrations at 60 °C. The surface exhibits a rough appearance with pyramidal hillocks of different sizes. The region between the hillocks seems to be flat, but a closer view shows that smaller hillocks decorate the surface.

3. Hillocks in 1D

We have performed a systematic study of the hillock formation in 1D through Monte Carlo simulations for a variety of site-specific rate constants using a restricted solid-on-solid model [17,18]. We focused specifically on the mechanisms that lead to the observed hillock-and-valley pattern (we mean by a valley a flat region between hillocks). In particular we determined the hillock number and size distribution within this landscape. Our simulations showed that the temporal evolution of the surface is controlled by hillocks that are continuously formed and annihilated and that they can grow and shrink. Based on these results, we concluded that hillock distributions are determined by four basic mechanisms: the valley etching, hillock etching, apex creation, and apex annihilation.

We proposed that the hillock-and-valley pattern emerges when hillocks are etched slightly faster than valleys, and then the hillock size distribution follows a decaying function with an exponential form. When the surface reaches a steady-state morphology, i.e. the hillock size distribution is stable, the number of hillocks per unit time of width w that grow to become hillocks of width $w + 1$ must be the same than the number of hillocks per unit time of width $w + 1$ that are etched to become hillocks of width w . Indeed, Monte Carlo modeling shows an exponentially decreasing distribution function for hillock sizes in 1D [18], evidence in favor of the interpretation given for the site-specific etching model of Ref. [19].

In our Monte Carlo modeling, a one-dimensional vector of 1000 sites represents the step. Periodic boundary conditions are used to avoid edge effects. Sites are visited at random and the detachment

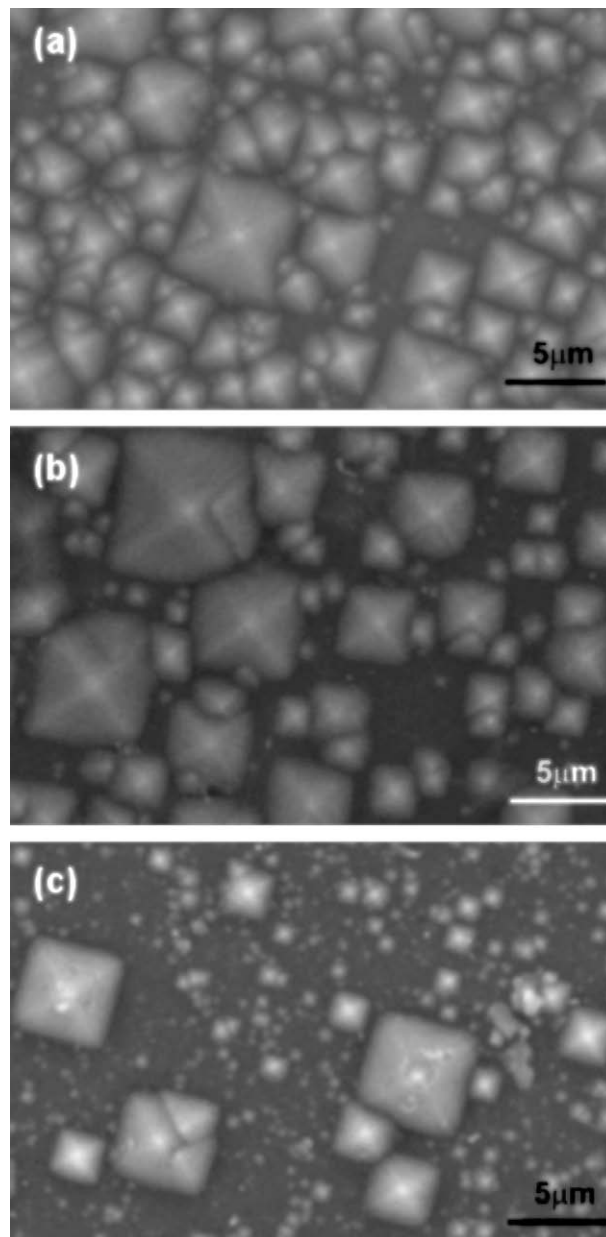


Fig. 1. Hillocks on a Si(1 0 0) surface etched in 1 M (a), 2 M (b), and 4 M (c) KOH during 2 h at 60 °C.

probability is determined according to its site-specific rate. The system evolves with successive annihilations of substrate particles until it approaches a steady-state configuration. We check that steady state is reached by monitoring the surface roughness evolution. Our simulation is based on the *restricted solid-on-solid* (RSOS) model in which there are no overhangs and a maximum height difference of one between neighboring columns is allowed. This condition assures the stability of hillock faces and ridges.

If only first neighbor interactions are considered and surface diffusion is not allowed, the parameters that determine the morphology in 1D are the removal rates of three distinct sites related to the particle coordination number. Particles available to be removed could have two (step site), one (kink), or zero (point site or apex) first neighbors along the step with etch rates k_i , where i is the coordination number. $k_{1,2}$ reflects substrate strength related to the number of first neighbor bonds, whereas k_0 includes a factor to take into account micromasking. Since we are interested in the

steady-state morphology, only the ratios of these parameters are relevant. Thus, adopting the value of $k_1 = 1$, the model has only two parameters: k_0 and k_2 .

Recently we developed a mean field model that reflects very well the general trends observed in the simulations [16]. With a model of this type we can readily estimate the impact of changing the relevant parameters on the resulting morphology without performing any computer simulation. In Fig. 2 we present the resulting hillock-and-valley widths derived from our mean field model as a function of k_0 for three values of k_2 . As expected, the size of the hillocks decreases with k_0 , since they are etched faster, and the valleys become wider. Also, for a given value of k_0 , the size of the hillocks increases with k_2 while the valleys become narrower. This can also be easily predicted because a larger k_2 implies a weaker substrate and then a faster valley etching. However, to predict the values of the parameters for a specific pattern in which, for example, hillocks and valleys have the same average size is not straightforward.

4. Hillocks in 2D

We have studied the hillock formation in 2D substrates through Monte Carlo simulations for a variety of site-specific rate constants within a restricted solid-on-solid model using a Kossel crystal [14,15]. In Fig. 3 we show hillock size distribution functions found for patterns obtained through Monte Carlo modeling. Distribution functions were obtained from four samples of 200×200 sites with a particle detachment probability given by $k_n = \exp(-nE/kT)$, where n is the number of first neighbors. According to this rule, an apex (a particle without neighbors) should be detached with probability equal to $k_0 = 1$. However, as previously stated, micromasking was incorporated in the model introducing a factor allowing k_0 to adopt smaller values. In particular, we present results corresponding to $E/kT = 2.3$ and $k_0 = 0.01, 0.014$. Note that hillock size distribution functions can be well fitted with exponentially decreasing functions.

From experimental observations, it can be found that hillock formation is affected by several factors such as etchant concentration, temperature, etchant agitation, and the presence of gases dissolved in the solution. In Fig. 4 we present the hillock size distribution obtained from experiments after etching Si(1 0 0) at

60 °C for three different etchant concentrations (namely 1, 2, and 4 M). From the analysis of the experimental data we checked that the hillock size distributions show a clear decreasing exponential dependence, as predicted by the MFM. To obtain these distribution functions the number of hillocks within a range around specific values were counted. The total density can be easily obtained by summing hillock densities for every size. Since the resulting distribution functions are decreasing exponentials, the inverse of the slope in a log-linear plot is the average hillock size (see Table 1). Consistently with the literature, we found that the hillock density decreases with etchant concentration [5]. We could also determine that the average hillock size is weakly affected by the etchant concentration.

Using a simple geometric argument, we can connect the total hillock density n with the average hillock size, w , and the average distance between hillock bases, a , which is an extension to 2D of the definition for the valley width given for 1D [16]:

$$n = \frac{1}{(a + w)^2}. \quad (1)$$

With Eq. (1) we can estimate a (see Table 1). We found that with etchant concentration both w and a increase. We have shown that increasing the apex etching rate or decreasing the stiffness of the substrate have the same effect in 1D (see Fig. 2) and in 2D (see Ref. [18]). Following [16], one can expect that the higher the etchant concentration the higher the removal probabilities at any site. However, etching is not uniformly affected but the effect is such that the rates corresponding to rapid etching sites are more affected. Since we are studying steady-state morphologies, the relevant quantities are the ratios between rates and not their absolute values. Therefore, an increase in the etchant concentration is equivalent to have a stiffer substrate.

Experiments show that w and a can increase or decrease simultaneously. Fig. 2 shows how this can be accomplished within the 1D mean field model. By simultaneously reducing k_0 and k_2 , as shown, hillocks become slightly larger and valleys considerably wider. A slight increase in average hillock sizes observed experimentally as a function of etchant concentration can be mimicked

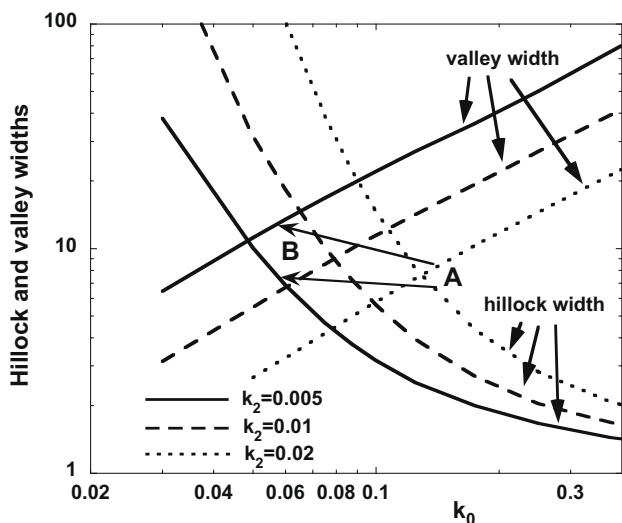


Fig. 2. Average widths of hillocks and valleys as a function of k_0 determined from the mean field model of Ref. [16]. Hillock sizes decrease with k_0 and increase with k_2 while valleys show the opposite trend. By changing both parameters k_0 and k_2 , the width of hillocks and valleys can increase (from A to B) or decrease (from B to A) simultaneously.

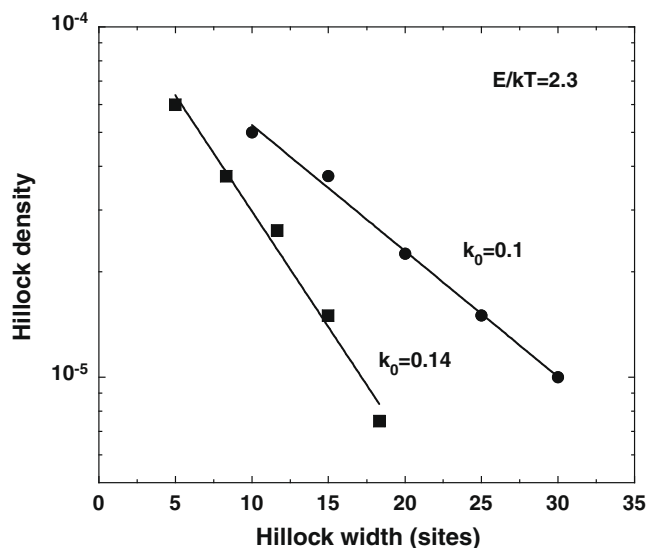


Fig. 3. Hillock size distribution functions (number of hillocks per site and width range) found through Monte Carlo modeling in 2D substrates. Particle detachment probabilities are given by $\exp(-nE/kT)$, where n is the number of first neighbors and $E/kT = 2.3$. Micromasking is incorporated in the model by reducing the value of k_0 , the detachment probability of an apex. Distributions show a decreasing exponential dependence.

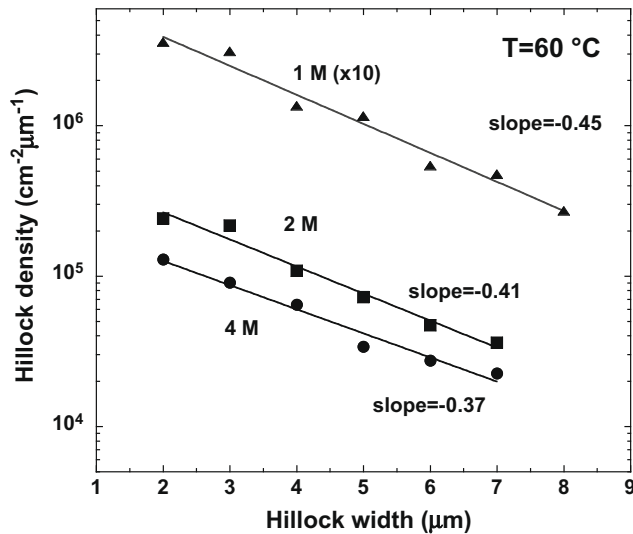


Fig. 4. Hillock density as a function of hillock width for Si(1 0 0) surfaces etched in 1, 2, and 4 M KOH during 2 h at 60 °C (symbols). For the sake of clarity, the distribution corresponding to 1 M was multiplied by a factor 10. Distributions are very well fitted with decreasing exponential functions (solid lines). This hillock size distribution indicates that hillock etching is faster than valley etching.

Table 1

Experimental hillock density and average hillock size as a function of etchant concentration for $T = 60$ °C.

KOH concentration	1 M	2 M	4 M
Hillock density (cm^{-2})	2.3×10^6	1.5×10^6	7.1×10^5
Average hillock size (μm)	2.2	2.4	2.7
Average valley size (μm)	4.5	5.8	9.1

with our model altering both parameters simultaneously as shown in Fig. 2 (from A to B), namely from $k_0 = 0.14$ and $k_2 = 0.02$ to $k_0 = 0.06$ and $k_2 = 0.005$.

5. Conclusions

A simple site-specific etching model can lead to the appearance of hillock-and-valley patterns observed in one- and two-dimen-

sional substrates. This model predicts that a hillock-and-valley pattern is possible under steady state if hillock etching is slightly faster than valley etching. This condition implies that the hillock size distribution must be an exponential decreasing function. In this work, we checked that experimental morphologies show exponential hillock size distributions according to the model prediction. In this letter, we also present the effect of etchant concentration on the hillock density and size distribution.

Acknowledgments

This work was partially supported by the CONICET (Argentina) and the ANPCyT (Grant No. 16-2500, Argentina).

References

- [1] M. Elwenspoek, H. Jansen, Silicon Micromachining, Cambridge University Press, Cambridge, 1998.
- [2] L.M. Landsberger, S. Naseh, M. Kahrizi, M. Paranjape, J. Microelectromech. Syst. 5 (1996) 106.
- [3] T. Baum, D.J. Schiffrin, J. Micromech. Microeng. 7 (1997) 338.
- [4] E. van Veenendaal, K. Sato, M. Shikida, J. van Suchtelen, Sensor. Actuat. A 93 (2001) 219.
- [5] S. Tan, M.L. Reed, H. Han, R. Boudreau, J. Microelectromech. Syst. 5 (1996) 1057.
- [6] H. Schröder, E. Obermeier, A. Steckenborn, J. Micromech. Microeng. 9 (1999) 139.
- [7] D. Cheng, M.A. Gosálvez, T. Hori, K. Sato, M. Shikida, Sensor. Actuat. A 125 (2006) 415.
- [8] D.B. Lee, J. Appl. Phys. 40 (1969) 4569.
- [9] R.A. Wind, M.A. Hines, Surf. Sci. 460 (2000) 21.
- [10] J. Flidr, Y. Huang, M.A. Hines, J. Chem. Phys. 111 (1999) 6970.
- [11] M.A. Gosálvez, K. Sato, A.S. Foster, R.M. Nieminen, H. Tanaka, J. Micromech. Microeng. 17 (2007) S1.
- [12] A.J. Nijdam, E. van Veenendaal, H.M. Cuppen, J. van Suchtelen, M.L. Reed, J.G.E. Gardeniers, W.J.P. van Enckevort, E. Vlieg, M. Elwenspoek, J. Appl. Phys. 89 (2001) 4113.
- [13] S.A. Campbell, K. Cooper, L. Dixon, R. Earwaker, S.N. Port, D.J. Schiffrin, J. Micromech. Microeng. 5 (1995) 209.
- [14] J. Flidr, Y. Huang, T.A. Newton, M.A. Hines, J. Chem. Phys. 108 (1998) 5542.
- [15] T.A. Newton, Y. Huang, L.A. Lepak, M.A. Hines, J. Chem. Phys. 111 (1999) 9125.
- [16] M.A. Gosálvez, R.M. Nieminen, New J. Phys. 5 (2003) 100.
- [17] M.P. Suárez, D.A. Mirabella, C.M. Aldao, Surf. Sci. 599 (2005) 221.
- [18] M.P. Suárez, D.A. Mirabella, C.M. Aldao, J. Mol. Cat. A 281 (2008) 230.
- [19] D.A. Mirabella, M.P. Suárez, C.M. Aldao, Surf. Sci. 602 (2008) 1572.
- [20] P. Raisch, W. Raisch, R.J. Nichols, D.J. Schiffrin, Electrochimica Acta 45 (2000) 4635.